Chemical Engineering Journal 111 (2005) 105–117

Chemical Engineering Journal

www.elsevier.com/locate/cej

Applications of polydisperse sedimentation models

Stefan Berres [a], Raimund Bürger [a,*], Elmer M. Tory [b]

[a] *Institut für Angewandte Analysis und Numerische Simulation, Universität Stuttgart, Pfaffen-waldring 57, D-70569 Stuttgart, Germany*
[b] *Mount Allison University, Sackville NB E4L 1E8, Canada*

Abstract

This paper reviews some recent advances in mathematical models for the sedimentation of polydisperse suspensions. Several early models relate the settling velocity to the solids concentration for a monodisperse suspension. Batchelor's theory for dilute suspensions predicts the settling velocity in the presence of other spheres that differ in size or density. However, this theory is based on the questionable assumption that identical spheres have identical velocities, and leads to significantly differing results for spheres that differ only slightly in size or density. Since Batchelor's analysis cannot be extended to concentrated suspensions, one needs to revert to semi-empirical equations and computational results. A rational model developed from the basic balance equations of continuum mechanics is the Masliyah–Lockett–Bassoon (MLB) model. A useful tool for evaluating polydisperse hindered settling models in general is a stability analysis. Basically, a model should reflect that, for polydisperse suspensions of equal-density spheres, instabilities such as blobs or fingers during separation are never observed. These structures do not form if the model equations are hyperbolic. The MLB model provably has this property, in contrast to certain extrapolations of the Batchelor model. The sedimentation process of a suspension can be simulated by either solving the conservation equations numerically by using a sophisticated scheme for conservation laws, or by using a particle-based method. Numerical examples illustrating both methodologies are presented, with an emphasis on fluidization problems.
© 2005 Elsevier B.V. All rights reserved.

Keywords: Polydisperse suspension; MLB model; Batchelor model; Fluidization

1. Introduction

Despite the attention paid to sedimentation of monodisperse suspensions, polydisperse suspensions are far more common. Some spheres are so nearly uniform that they are essentially identical [1–3]. However, many experiments with "monodisperse suspensions" involve spheres that have an approximately normal distribution with a considerable spread in diameters [4,5]. Similarly, each species in a "bidisperse" or "tridisperse" suspension often has a distribution of diameters [6].

The relationship between settling velocity and solids concentration in monodisperse suspensions has been the subject of many theoretical and empirical studies. Noting that the presence of particles affects both the density and viscosity of the suspension (see, for example, [7]), Robinson [8] suggested, as early as 1926, a modification of Stokes' law in which the density and viscosity of the suspension replace those of the fluid. For very dilute suspensions, Kermack et al. [9] and Batchelor [10] derived equations of the form

$$v(\phi) = u_\infty(1 - n\phi), \tag{1}$$

where v is the velocity of a sedimenting sphere,

$$u_\infty = -\frac{\Delta\rho g d^2}{18\mu_\mathrm{f}} \tag{2}$$

is the Stokes velocity (where $\Delta\rho$ is the solid–fluid density difference, g the acceleration of gravity, d the diameter of the sphere and μ_f is the dynamic viscosity of the fluid), and ϕ is the volumetric solids concentration. There are many empirical or semi-empirical equations such as those of Steinour [11], Richardson and Zaki [12], and Barnea and Mizrahi [13]. Of these, the best known and most widely used is the

* Corresponding author. Present address: Departmento de Ingeniería Matemática, Universidad de Concepción, Casilla 160-C, Concepción, Chile. Tel.: +49 711 6857647; fax: +49 711 6855599.

E-mail addresses: berres@mathematik.uni-stuttgart.de (S. Berres), buerger@mathematik.uni-stuttgart.de (R. Bürger), sherpa@nbnet.nb.ca (E.M. Tory).

1385-8947/$ – see front matter © 2005 Elsevier B.V. All rights reserved.
doi:10.1016/j.cej.2005.02.006

Richardson–Zaki equation

$$u(\phi) = u_\infty(1-\phi)^n. \quad (3)$$

Eq. (3) is often used for slightly polydisperse suspensions. Then, the value of u_∞ is determined by extrapolation and compared to the value calculated for some representative diameter [4,14]. The value of n depends on the Reynolds number and, to a lesser extent, on the sphere–cylinder diameter ratio. Most experimental values range from 4.6 to 5.5 for creeping flow. Scott [15] suggests 4.7 as the most appropriate value. The reasons for the considerable variation are not entirely understood, so n is appropriately chosen as the value that gives the best fit.

2. Sedimention of dilute suspensions

Kermack et al. [9] in 1929 appear to have been the first to use the condition that the net flux in batch sedimentation is zero. In modern terminology:

$$q = (1-\phi)v_\mathrm{f} + \phi_1 v_1 + \cdots + \phi_K v_K = 0, \quad (4)$$

where q is the volume–average velocity of the suspension, v_f the velocity of the fluid, ϕ_k and v_k the volume fraction and the velocity of solids species k, $k = 1, \ldots, K$, and $\phi = \phi_1 + \cdots + \phi_K$ is the total solids volume fraction. Condition (4) is obvious for a contained suspension and serves as the definition of batch sedimentation. Since increasing the size of a cluster increases its velocity, Eq. (4) must be imposed on an unbounded suspension to obtain a finite velocity. Batchelor [10] also used $q = 0$ in his derivation of the mean particle velocity in a monodisperse suspension. Unlike many others, who assumed a lattice or some other ordered configuration, he assumed that the suspension was disordered. This assumption has been confirmed by many direct observations [16–18]. Batchelor's major contribution was his recognition of the importance of the deviatoric stress tensor:

$$d_{ij} = \sigma_{ij} - \tfrac{1}{3}\delta_{ij}\sigma_{kk}, \quad (5)$$

which is defined in both the fluid and solid parts of the dispersion and has the Newtonian form $2\mu_\mathrm{f} e_{ij}$ in the fluid, where e_{ij} is the rate of strain tensor. In Eq. (5), δ_{ij} is the Kronecker delta. Batchelor noted that $d_{ij}(\mathbf{x})$ is a stationary random function of position in a statistically homogeneous suspension, and so has constant mean. After an extensive analysis using these assumptions and the probability distribution of the separation of two spheres, he obtained Eq. (1). He noted that assuming an ordered structure led to a completely different dependence on ϕ, namely $\phi^{1/3}$. He also recognized that the value of n depends on the assumed distribution of sphere centers.

A similar analysis of polydisperse suspensions [19,20] led to

$$v_i = u_{\infty i}(1 + S_{i1}\phi_1 + \cdots + S_{iK}\phi_K), \quad i = 1, \ldots, K, \quad (6)$$

where $u_{\infty i}$ is the Stokes velocity of the ith species, ϕ_j the concentration of the jth species, and the coefficients S_{ij} are the so-called "Batchelor coefficients". While Batchelor and Wen [20] calculated results for many different combinations of size and density, the values for identical and nearly identical spheres are of special interest because they highlight the importance of their assumptions. They obtained the values $S_{ii} = -6.55$ for $\lambda = 1$ and $\gamma = 1$, $S_{ii} = -5.6$ for $\lambda \approx 1$ and $\gamma = 1$ and $S_{ii} = -2.6$ for $\lambda = 1$ and $\gamma \approx 1$, where $\lambda := d_j/d_i$, $\gamma := (\rho_j - \rho_\mathrm{f})/(\rho_i - \rho_\mathrm{f})$, d_i and ρ_i are the size and the density of species i, respectively, and ρ_f is the density of the fluid. These strange results arise from their assumption that identical spheres have identical velocities while spheres that differ slightly in either size or density have slightly different velocities. Tory and Kamel [3] pointed out that identical spheres do not have identical velocities [17]. Indeed, the effects of very small differences in size and/or density are completely dwarfed by the huge influence of local configuration [1,16,18,21]. This throws into question Batchelor's markedly different results for almost identical situations. Indeed, Tory and Kamel [3] maintain that hydrodynamic diffusion makes the cases ($\lambda = 1$, $\gamma = 1$), ($\lambda \approx 1$, $\gamma = 1$), ($\lambda = 1$, $\gamma \approx 1$), and ($\lambda \approx 1$, $\gamma \approx 1$) essentially the same.

In fact, all of these cases at large Peclet numbers must be compared with the Richardson–Zaki equation for small values of ϕ. Batchelor's equation (with $S_{ii} = -6.5$ for $\lambda \approx 1$, $\gamma \approx 1$) appears to work well at small Peclet numbers in the absence of interparticle forces [2]. In this case, Brownian motion ensures that the random distribution of sphere centers remains uniform. Hydrodynamic diffusion is very important at large Peclet numbers, but is not taken into account in the Batchelor–Wen analysis. Since this diffusion depends on some regions of the suspension being denser than others [21], the steady-state distribution is not obvious. A further difficulty is that Eq. (6) applies only to very dilute suspensions, but this is the range in which "cluster settling" occurs [1,22–24]. Hence, calculated and measured velocities may not agree [3], especially when the diameter of the container is large compared to the particle diameter [23,25]. Typically, the interface velocity is less than the mean velocity of the spheres in the interior [1,26], which may be greater than the Stokes velocity [24,26].

3. Sedimentation at higher concentrations

Eq. (4) and the condition on $d_{ij}(\mathbf{x})$ apply at all concentrations, but the type of analysis used by Batchelor applies only to dilute suspensions. Geigenmüller and Mazur [27] studied the sedimentation of spherical particles of common diameter d in an incompressible fluid of viscosity μ_f in a closed container. Starting from the pressure tensor in the fluid they showed that the friction force that the fluid exerts on a sphere *in a suspension* equals the buoyancy-corrected gravitational force on it. For a polydisperse suspension, this is

$$\int \mathbf{F}_k(\mathbf{r})\,\mathrm{d}\mathbf{r} = \frac{\pi}{6} d_k^3(\rho_k - \rho_{\mathrm{f}})\mathbf{g}. \tag{7}$$

Note that they use the density of the fluid, not the suspension. This distinction is important in view of the controversy surrounding the use of the suspension density in sedimentation and fluidization [28]. Of course, $\mathbf{F}_k(\mathbf{r})$ depends on $\Phi = (\phi_1, \phi_2, \ldots, \phi_K)^{\mathrm{T}}$, the vector of solids concentrations of the K species. In principle, the derivation by Geigenmüller and Mazur yields velocities for concentrated suspensions, but the solution rapidly becomes intractable for non-dilute suspensions. Thus, empirical equations or computational results are required at higher concentrations.

Davis and Gecol [29] postulated that Batchelor's results could be extended to higher concentrations. They introduced the equation

$$v_i = u_{\infty i}(1-\phi)^{-S_{ii}} \left(1 + \sum_{j=1}^{K} (S_{ij} - S_{ii})\phi_j\right), \quad i = 1, \ldots, K. \tag{8}$$

This simplifies to Eq. (3) for monodisperse suspensions (with $n = -S_{ii}$). For very small values of ϕ, terms of second order can be neglected, and Eq. (8) reduces to Eq. (6). Richardson and Shabi [30] stated that the settling velocities in a polydisperse suspension could be represented as

$$v_k = u_{\infty k}(1-\phi)^n, \quad k = 1, \ldots, K. \tag{9}$$

However, this equation does not adequately account for differences in the return flow of fluid caused by the downward movement of different species. The appropriate generalization of the Richardson–Zaki equation is the Masliyah–Lockett–Bassoon (MLB) equation [31–33]:

$$v_k = \mu(1-\phi)^{n-2} \times \left(\delta_k(\rho_k - \rho(\Phi)) - \sum_{j=1}^{K} \delta_j \phi_j (\rho_j - \rho(\Phi))\right), \quad k = 1, \ldots, K, \tag{10}$$

where

$$\rho(\Phi) := \rho_{\mathrm{f}}(1-\phi) + \rho_1\phi_1, + \cdots + \rho_K\phi_K, \tag{11}$$

$$\delta_k := \frac{d_k^2}{d_1^2}, \qquad \mu := -\frac{g d_1^2}{18\mu_{\mathrm{f}}} = \frac{u_{\infty 1}}{\rho_1 - \rho_{\mathrm{f}}}. \tag{12}$$

Here, $u_{\infty 1}$ is the Stokes velocity of the largest species. Note that $u_{\infty 1} < 0$ when $\rho_1 - \rho_{\mathrm{f}} > 0$. As in the Richardson–Zaki equation, the value of n can be chosen to fit the experimental data [34].

Contrary to the statement in a recent review [35], Masliyah did not assume that "the slip velocity (velocity of particle relative to the liquid) is governed by the . . . and the difference between the particle and suspension densities". Of course, Eq. (10) shows that $\rho_k < \rho(\Phi)$ and $\rho_j > \rho(\Phi)$, $j \neq k$, imply that the kth species will indeed move upwards. However, this result is not an assumption, but a consequence.

The fundamental assumption for the rigorous derivation [33,36] of the MLB [31,32] and the related Patwardhan–Tien model [37] is that the solid–fluid interaction force between the ith species and the fluid is given by a concentration-dependent factor multiplying the slip velocity, or solid–fluid relative velocity $v_i - v_{\mathrm{f}}$. (This approach is in agreement with the principle of objectivity, which states that constitutive equations should be stated in terms of objective quantities, and it is well known that the difference between two velocities is objective, while a single velocity is not [38].) Inserting these assumptions into the reduced momentum balances for each solids species and the fluid and choosing a Richardson–Zaki [12] dependence, viz.

$$V(\Phi) = \begin{cases} (1-\phi)^{n-2} & \text{if } 0 \le \phi \le \phi_{\max}, \\ 0 & \text{otherwise}, \end{cases} \tag{13}$$

we unequivocally obtain Eq. (10). Nevertheless, Ha and Liu [39] state that the main assumption of models based on slip velocities is that "the particle volume fractions are uniform in any given region". This is incorrect, of course. Moreover, it betrays a fundamental misunderstanding of the nature of models. A model is simply a means of predicting settling velocities from solids concentrations, i.e., $v(\Phi)$. It is beyond the scope of modeling to assume that the concentrations are uniform in any given region; the concentrations are determined by the evolution of the suspension. In some cases, the concentrations remain constant in a certain region; in other cases, they do not.

Finally, we mention that it is necessary to explicitly "build in" to the mathematical model that the solution should assume physically relevant values only. This is most conveniently done by setting the hindered settling factor to zero wherever necessary, as is done in Eq. (13).

When $\rho_1 = \rho_2 = \cdots = \rho_K$, Eq. (10) reduces to

$$v_k = v_k(\Phi) = u_{\infty 1}(1-\phi)^{n-1}(\delta_k - (\delta_1\phi_1 + \cdots + \delta_K\phi_K)), \quad k = 1, \ldots, K \tag{14}$$

as the velocity of the kth species [40]. Eq. (14) clearly reduces to Eq. (3) when only a single species is present. Thus, Eqs. (3), (14) and (10) represent a consistent, unified approach to sedimentation.

Patwardhan and Tien [37] proposed a model in which the effective solids concentration is different for each species. This could be more accurate if steric hindrance causes some small particles to be carried downward with the larger ones rather than moving freely in the liquid. However, as noted below, it makes the analysis of stability more difficult.

4. Stability of suspensions

Analyses of settling suspensions are usually one-dimensional, so it is important to identify suspensions in which a three-dimensional analysis is required. Thanks largely to the work of Weiland and his collaborators [41–43], it became apparent that suspensions of particles of greatly differing densities settle in an anomalous manner. In particular, instability phenomena such as blobs and fingering are evident. In the most extreme cases, bidisperse suspensions of heavy and buoyant particles segregate into upward and downward streams, resulting in a much faster separation than that predicted from a one-dimensional analysis.

Batchelor et al. [44] formulated a stability criterion for bidisperse suspensions. Biesheuvel et al. [45] used this criterion to test the predictions of the MLB and Patwardhan–Tien models. Using the MLB and Davis–Gecol models, Bürger et al. [33] showed that some flux-density vectors

$$\mathbf{f}(\Phi) = (f_1(\Phi), f_2(\Phi), \ldots, f_K(\Phi))^{\mathrm{T}}$$

cause the first-order system of conservation laws

$$\frac{\partial \phi_i}{\partial t} + \frac{\partial f_i(\Phi)}{\partial x} = 0, \quad i = 1, \ldots, K \tag{15}$$

to be non-hyperbolic, or to be of mixed hyperbolic–elliptic type in the bidisperse case. The criterion for ellipticity is equivalent to the stability criterion. They showed that loss of hyberbolicity, indicated by the occurrence of complex eigenvalues of the Jacobian of Eq. (15)

$$\mathbf{J_f}(\Phi) := \left(\frac{\partial f_i(\Phi)}{\partial \phi_k}\right)_{i,k=1,\ldots,K}, \tag{16}$$

can be viewed as an instability criterion for arbitrary polydisperse systems. For tridisperse suspensions, this criterion can be evaluated by a convenient calculation of a discriminant. Bürger et al. [33] proved that the MLB equation predicts stability for all bidisperse suspensions in which the spheres have the same density, and conjectured that all polydisperse suspensions of this kind would be stable. This conjecture was proved by Berres et al. [36]. The generic assumption to ensure hyperbolicity and hence stability is

$$V(\phi) > 0, \qquad V'(\phi) < 0 \quad \text{for} \quad 0 < \phi < \phi_{\max}, \tag{17}$$

where $\phi_{\max}$ is the maximum total solids concentration feasible in the polydisperse system. Thus, the form shown in Eq. (14) is not the only one that ensures stability. However, Eq. (17) is satisfied by $V(\phi) = (1 - \phi)^{n-2}$, $n > 2$, and, as noted above, this form is consistent with the Richardson–Zaki equation. The important point is that the proof at present is limited to functions of the form $V(\phi)$ only. Specifically, it is not clear to us at the moment whether it may be extended to the hindered settling factors of the Patwardhan–Tien model [37], which depend on Φ rather than ϕ, and differ for each particle species. At present, this model appears to be too complicated for generalizations of the stability analysis in [33,36], so only numerical calculations are possible.

In contrast to the MLB equation, the Davis–Gecol equation predicts regions of instability for some bidisperse systems in which both species have the same density [33]. As there is no creditable experimental evidence for such instability, the Davis–Gecol equation is inferior to the MLB equation in this respect. It seems to us that these qualitative predictions are extremely important. For example, if some degree of instability is present in a bidisperse system in which $\rho_1 > \rho_2 > \rho(\Phi)$, species 1 may stream through species 2 as both move downward. Then, we should not expect agreement with results from a one-dimensional analysis. Thus, simple comparisons of calculated and experimental results are an inadequate criterion for evaluating models when particle densities differ substantially. Comparisons of experimental and theoretical results for an equal-density case are always appropriate. However, such comparisons should be based on the entire settling curves and, if possible, the rise of the packed bed. In this regard, we note that recent work by Bargieł et al. [34] shows close agreement between Eq. (14) and the experimental results of Shannon et al. [4,46]. See Section 8 for the risks involved in using a cited concentration dependence as the only basis for evaluation of models [35].

5. The sedimentation process

Sedimentation is the evolution of $\Phi(z,t)$, $0 < z \le H$, $t \ge 0$, from Φ^0 to $\Phi_{\max}(z)$, where $\Phi_{\max}$ is the value of Φ when $\phi = \phi_{\max}$. This evolution is governed by the solids flux vector $\mathbf{f} = (f_1, f_1, \ldots, f_K)^{\mathrm{T}}$, where $f_k = \phi_k v_k$. The two essentials for predicting this evolution are the model equation and a method of implementing the changes produced by the flux. The global behavior of sedimenting monodisperse suspensions can be deduced from the flux plot [46–49], but this approach is not available for polydisperse suspensions. The settling process is still governed by the solids flux, but the process is more complicated. In particular, the evolution depends not only on the total flux $f = f_1 + f_2 + \cdots + f_K$, but also on the components f_k.

In one of the earliest treatments of a polydisperse suspension, Smith [50] derived the increases in the concentrations of slower-settling species in the upper regions. For simplicity, consider the sedimentation of a bidisperse suspension. The uppermost region contains only the slower settling species designated as species 2. Suppose that the solids concentrations of both species remain constant in the region above the packed bed. The faster settling species (designated by 1) is absent from the top level (designated by +). Thus, the velocity of species 2 there is $v_2(\phi_2^+)$. Below the mixed-small interface, the velocities are $v_2(\Phi^0)$ and $v_1(\Phi^0)$. A material balance [50] yields

$$\phi_2^+[v_2(\phi_2^+) - v_1(\Phi^0)] = \phi_2^0[v_2(\Phi^0) - v_1(\Phi^0)]. \tag{18}$$

Species 2 settles more rapidly in the upper region than in the original suspension. Since downward velocities are negative, $v_2(\phi_2^+) < v_2(\Phi^0)$. From Eq. (18), $\phi_2^+ > \phi_2^0$. This "Smith effect" can be seen in many simulations [34,36,40,51,52]. A similar derivation can be applied to any discrete polydisperse suspension. Bargieł et al. [34] derived the same result from an analysis of particle paths.

Successful prediction of suspension evolution requires that the scheme proceed automatically from Φ^0 to $\Phi_{\max}$. There are two main methods of implementing the theoretical evolution of the suspension. One is to use a sophisticated numerical scheme that tracks discontinuities automatically [36,53–55]. We briefly discuss these schemes, following the introduction of [52]. These schemes, which will produce accurate approximations of discontinuous solutions to Eq. (15) without explicitly using jump conditions or shock-tracking techniques, are called *shock-capturing*. The last three decades have seen tremendous progress in the development of shock-capturing schemes for systems of conservation laws; see for example [56,57]. Roughly speaking, shock-capturing schemes may be classified into two categories: central and upwind. The main disadvantage of upwind schemes is the difficulty of solving the Riemann problem exactly or approximately, especially for complicated systems of conservation laws. In fact, the (exact or approximate) solution of the Riemann problem for (15) combined with the flux vector defined by (10) has not yet been determined. For this reason, central schemes have so far been preferred. In the 1990s, this class of schemes received (in part renewed) interest following Nessyahu and Tadmor's [54] second-order sequel of the Lax–Friedrichs scheme. A general introduction to central schemes is given in [56]. However, the Kurganov–Tadmor scheme [53] is employed for the numerical examples in this paper. This modification of Nessyahu–Tadmor scheme has a smaller numerical viscosity and is better suited for nearly steady-state calculations.

The other method to implement the theoretical evolution of the suspension is to use a particle-based simulation [34,51]. In this scheme, the velocity of each particle is governed by the solids concentration in a thin region (of height h) immediately below that particle. The thickness, h, must be large enough to measure concentration accurately, but small enough to emphasize the concentration near the test particle. If the number of particles is very large, this region can be quite thin. To handle the lowest particles, we set $\phi = \phi_{\max}$ in an artificial region (of thickness h) below the bottom [48]. The particles in this region are uniformly distributed over h.

This specification of concentration has several advantages. It corresponds to the usual idea of the dependence of the interface velocity and ensures that the particles at the top of a uniformly mixed suspension settle with the same velocity as those in the bulk of the suspension. It also incorporates the fact that a particle approaching a flat plate or a fixed bed slows down [58–61]. Finally, it recognizes that a dense region above a dilute one settles rapidly into or through the latter [1,18].

This scheme works as follows: The particles are initially distributed uniformly over the total height of the column. In the first time-step, all particles (of a given species) above h have the same velocity, but those below settle more slowly because they are affected by particles in the artifical sublayer. The lowest particle is in the region where the effective concentration is the greatest, so it will settle the slowest of any particles of its species. The next lowest particle of that species will settle slightly faster, and so on. Each step increases the concentration in $(0, h)$. If the time-step is sufficiently small, this soon produces a concentration gradient ranging from $\phi_{\max}$ at the bottom to ϕ_0. This is more realistic than Kynch's assumption that these concentrations form immediately [47]. The simulation can also handle an initially random distribution of particles. Additional details, including algorithms for both versions, are given in [34].

The simulation is very realistic in that concentrations are controlled directly by the solids flux. Where discontinuities are predicted from Kynch's theory, the simulations produce a very sharp continuous change. Concentration gradients expand in the usual way. Bargieł et al. [34] show settling curves for bidisperse suspensions and for a polydisperse approximation of a suspension with normal size distribution of diameters. Simulations involving several million particles are feasible. An example is shown in Section 8.

Though one can sometimes follow the evolution of Φ by measuring the rise of the discontinuity and using (18) or its generalization to calculate the concentrations in the upper levels, this method is unsatisfactory for two reasons. First, the method should automatically determine the positions of discontinuities. Second, the propagation of concentration gradients in the lower region may change the concentration at the top of that region [34], thereby invalidating the calculation of the concentrations in the upper levels. The important feature of the Kurganov–Tadmor scheme [53] and the particle-based simulation [34] is that they automatically follow the positions of discontinuities and also propagate concentration gradients where appropriate.

A sophisticated numerical scheme has been used to predict the sedimentation of compressible polydisperse suspensions [36]. Results for equal-density species are reasonable for the early stages of sedimentation, but some issues regarding the final stages have not yet been resolved. The case of compressible particles of different densities appears to be difficult because they will, in general, have different compressibilities [36].

6. Fluidization

Polydisperse sedimentation models can also be used to describe processes in which a relatively compact bed of particles is fluidized by an upwards bulk flow of fluid [62,63]. Complete mixing and bed inversion of bidisperse suspensions have long been of particular interest [37,64–67]. Berres et al. [62] established compatibility conditions for bidisperse systems and later [63] extended the analysis to tridisperse and higher discrete polydisperse systems. The basic result from [62,63], for simplicity presented here for a bidisperse suspension only, states that a necessary condition for the existence of a fluidized bed is that the following inequalities are satisfied

$$d_1 > d_2, \tag{19}$$

$$d_1^2(\rho_1 - \rho_f) > d_2^2(\rho_2 - \rho_f), \tag{20}$$

$$\rho_1 < \rho_2. \tag{21}$$

Assume that the material parameters are chosen such that (19)–(21) are satisfied. Then a completely fluidized bed made of these species can exist if its volume fractions (ϕ_1^*, ϕ_2^*) satisfy [62]

$$\phi_2^* = -\frac{\rho_1 - \rho_f}{\rho_2 - \rho_f}\phi_1^* + \frac{(\rho_2 - \rho_f)d_2^2 - (\rho_1 - \rho_f)d_1^2}{(d_2^2 - d_1^2)(\rho_2 - \rho_f)}. \tag{22}$$

Obviously, the set of all states (ϕ_1^*, ϕ_2^*) that satisfy (22) forms a straight line in a ϕ_1 versus ϕ_2 diagram. The corresponding fluidization velocity is given by

$$\begin{aligned} q^* = &-(1-\phi^*)\mu V(\phi^*)(-(1-\phi^*)\rho_f \\ &+\rho_1(1-\phi_1^*) - \rho_2\phi_2^*). \end{aligned} \tag{23}$$

According to our discussion of Section 4, the MLB model for bidisperse particles having different densities will in general give rise to a hyperbolic-elliptic system, that is, to instability regions in a ϕ_1 versus ϕ_2 diagram. In particular, these instability regions will exist for a bidisperse suspension satisfying (19)–(21). Furthermore, consider that the governing equation for fluidization of ideal suspensions is

$$\frac{\partial \Phi}{\partial t} + \frac{\partial}{\partial x}(q\Phi + \mathbf{f}(\Phi)) = 0. \tag{24}$$

Thus, the Jacobian relevant for the stability analysis is $q\mathbf{I} + \mathbf{J_f}(\Phi)$, where $\mathbf{J_f}(\Phi)$ is the Jacobian of the batch settling equation defined in (16). Since adding a multiple of the identity matrix does not change the nature of eigenvalues, the stability and instability regions for fluidization are the same as for batch settling.

One may raise the question whether the fluidized-bed steady states (ϕ_1^*, ϕ_2^*) may become unstable. Interestingly, it can be proved (see [63]) that, within the MLB model, the completely fluidized states are always stable. In other words, the line (22) avoids the ellipticity (instability) region. This will be illustrated in the next section.

Additional criteria are required to determine the sequence of mixtures in incompletely mixed beds (see [63]).

7. Numerical examples

In this section, we present three recent numerical examples illustrating the predictions of the MLB model for batch centrifugation of a tridisperse suspension, fluidization of a bidisperse suspension, and gravity separation of a bidisperse suspension. In all cases, the schemes utilized are variants of the Kurganov–Tadmor scheme [53]. For simulations of batch settling of polydisperse suspensions, we refer to some earlier papers [34,36,40,51,52,68].

7.1. Batch centrifugation of a polydisperse suspension

For tube or basket centrifuges rotating at an angular velocity ω, the MLB model and its extension to compressible sediments [36] again yield a spatially one-dimensional model (with the radius r as spatial coordinate) provided that ω is large enough that the influence of the gravitational compared to the centrifugal body force can be neglected, and ω is at the same time small enough that the effect of Coriolis forces is not dominant [69]. The analysis of a monodisperse, ideal suspension due to Anestis [70] and Anestis and Schneider [71] clearly shows that curved shocks appear when the solution of the centrifugation model is plotted, for example, by iso-concentration lines of the solids volume fraction in a time-versus-radius diagram, and that the suspension located between the suspension-sediment and suspension-clear liquid interfaces does not remain at the initial concentration; rather, its concentration decreases as a function of time.

We present here one recent example taken from [69] to illustrate the predictions for the MLB model including sediment compressibility. We consider a tridisperse suspension with particles made of the same material ($\rho_1 = \rho_2 = \rho_3 = 1800\,\mathrm{kg/m^3}$) and sizes $d_1 = 1.19 \times 10^{-5}\,\mathrm{m}$, $d_2 = 2^{-1/2}d_1$ and $d_3 = d_1/2$ that are suspended in a fluid with density $\rho_f = 1000\,\mathrm{kg/m^3}$ and viscosity $\mu_f = 10^{-3}\,\mathrm{Pa\,s}$. The suspension is assumed to initially fill a rotating tube with inner radius (suspension meniscus) 0.05 m and outer radius 0.15 m. The hindered settling factor is assumed to be given by (13) with $n = 4.7$ and a nominal maximum solids concentration $\phi_{\max} = 0.68$. (The solids concentration attained in the system is actually lower.) Though it is beyond the scope of this review to elucidate the model, we finally mention that the effective solid stress function accounting for sediment compressibility is

$$\sigma_e = \begin{cases} 0 & \text{for } \phi \le \phi_c, \\ \sigma_0\left(\left(\dfrac{\phi}{\phi_c}\right)^k - 1\right) & \text{for } \phi > \phi_c, \end{cases} \tag{25}$$

where the parameters take the values $\sigma_0 = 180\,\mathrm{Pa}$, $\phi_c = 0.2$ and $k = 6$. The centrifuge is assumed to rotate at an angular velocity $\omega = 25.573\,\mathrm{rad/s}$ and assumed to be filled initially with a suspension of concentration $\Phi^0 = (0.04, 0.04, 0.04)$. Fig. 1 shows the numerical simulation of the centrifugation process obtained by the Kurganov–Tadmor method [53].

7.2. Fluidization of a bidisperse suspension

Next, we present a new simulation of the fluidization of a bidisperse suspension studied by Moritomi et al. [66]. The relevant parameters are $\delta_2 = 0.04412$, $\rho_1 - \rho_f = 500\,\mathrm{kg/m^3}$ (hollow char particles) and $\rho_2 - \rho_f = 1450\,\mathrm{kg/m^3}$ (glass beads). Fig. 2 shows a plot of the instability (ellipticity) region for the MLB model for this system. Moreover, the points B, C, D, E and F lie on the straight line given by (22), and correspond to completely fluidized beds with the fluidization

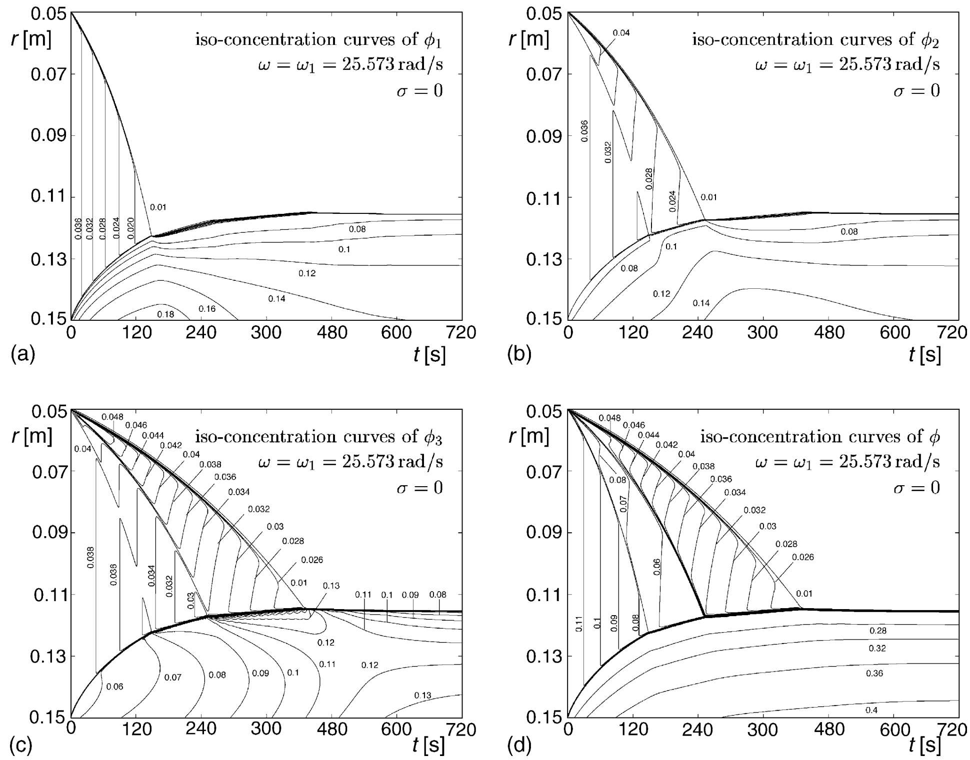

Fig. 1. Simulation of the centrifugation of a tridisperse suspension with compressible sediment [69] showing iso-concentration lines of (a) the largest, (b) the second-largest and (c) the smallest particles, and (d) of the cumulative solids volume fraction.

velocities $q_{\mathrm{B}} = 1.77 \times 10^{-6}$ m/s, $q_{\mathrm{C}} = 9.64 \times 10^{-4}$ m/s, $q_{\mathrm{D}} = 1.39 \times 10^{-3}$ m/s, $q_{\mathrm{E}} = 1.84 \times 10^{-3}$ m/s and $q_{\mathrm{F}} = 3.56 \times 10^{-3}$ m/s, respectively. We use this information to solve (24) numerically with the initial condition $\phi_1^0(x) = \phi_2^0(x) = 0.2$ for $0 \le x \le L = 1\,m$ and the boundary

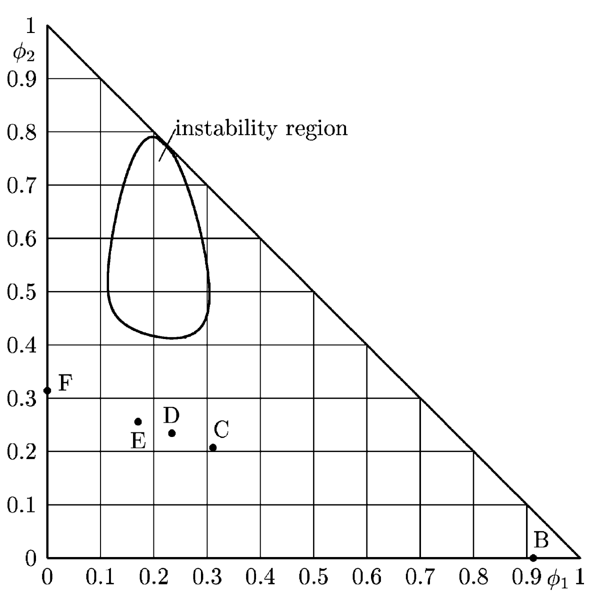

Fig. 2. The instability region for the MLB model and a bidisperse suspension studied by Moritomi et al. [66]. The collinear points B, C, D, E and F represent compositions of stationary fluidized beds at various fluidization velocities q_{B} to q_F.

condition $f|_{x=0} = 0$, and setting:

$$q = q(t) = \begin{cases} 0 & \text{for } 0 \le t \le 1500\,\mathrm{s}, \\ q_{\mathrm{C}} & \text{for } 1500\,\mathrm{s} < t \le 3000\,\mathrm{s}, \\ q_{\mathrm{D}} & \text{for } 3000\,\mathrm{s} < t \le 4500\,\mathrm{s}, \\ q_{\mathrm{E}} & \text{for } 4500\,\mathrm{s} < t \le 5500\,\mathrm{s}, \\ q_{\mathrm{D}} & \text{for } t > 5500\,\mathrm{s}. \end{cases} \qquad (26)$$

Note that for $t \le 1500$ s, we apply no fluidization velocity and thus batch settling occurs. Fig. 3 shows the numerical result for this stage by a sequence of Lagrangian paths, that is, the trajectories of the particles separating the lowest 1%, 10%, 20%, ..., 90%, 99% from the remaining particles of the species considered. Fig. 4 shows Lagrangian paths for the complete fluidization process, while Figs. 5 and 6 depict the concentration distribution for species 1 and 2, respectively. We observe that each time q is increased, both species initially move upwards before gradually attaining their steady-state positions.

7.3. Gravity separation of polydisperse suspensions

In a series of papers, Nasr-El-Din et al. [73–75] report experimental results and present a limited mathematical treatment for gravity separation of polydisperse systems with particles differing in density. The basic equipment is a vertical column equipped with a surface source through which feed suspension is fed into the unit. The desired mode

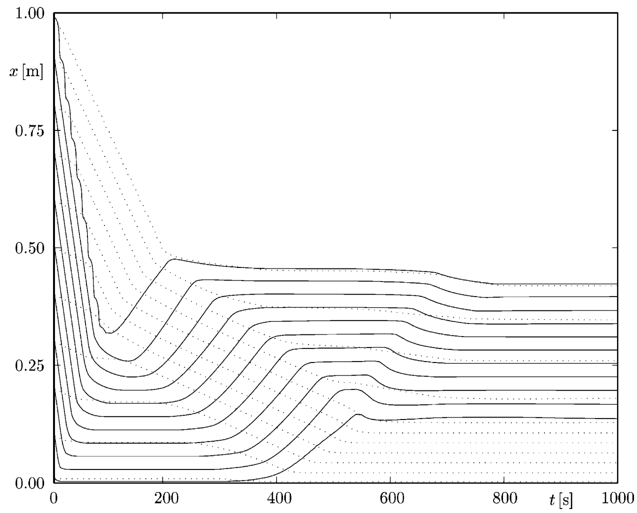

Fig. 3. Simulation of the settling of a bidisperse suspension with parameters chosen according to Moritomi et al. [66]. The solid and dotted lines are Lagrangian paths of species 1 and 2, respectively.

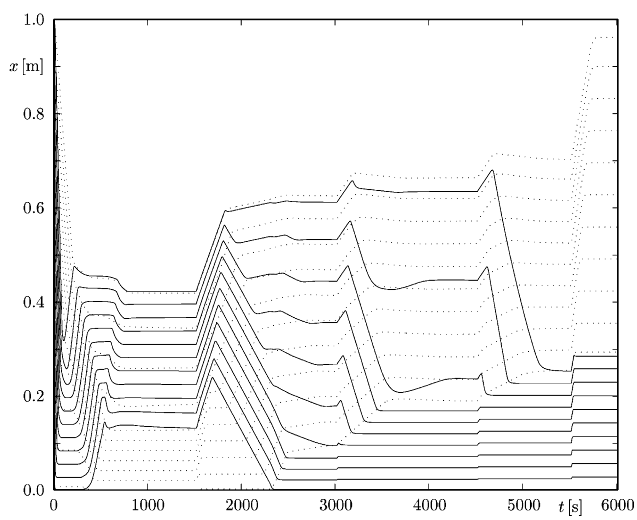

Fig. 4. Fluidization of a bidisperse suspension with parameters chosen according to Moritomi et al. [66] and a stepwise increased fluidization velocity $q(t)$ given by (26).

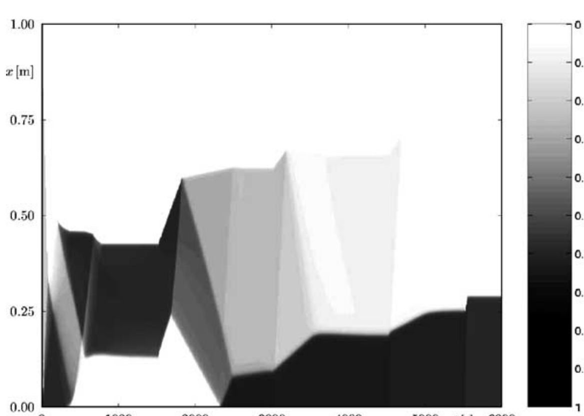

Fig. 5. Fluidization of a bidisperse suspension with parameters chosen according to Moritomi et al. [66]: concentration of species 1.

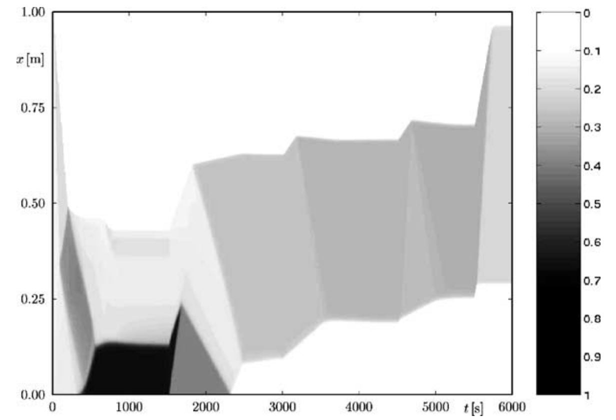

Fig. 6. Fluidization of a bidisperse suspension with parameters chosen according to Moritomi et al. [66]: concentration of species 2.

of operation is that the upwards-directed flow in the column carries the lighter and the downwards-directed flow the heavier particles. Such an idealized clarifier-thickener is drawn in Fig. 7, which is supposed to have a constant cross-sectional area S. This unit is supposed to treat a polydisperse suspension, and is operated in the following way, where we assume that x is downwards increasing. At depth $x = 0$, feed suspension is fed into the equipment at a volume rate $Q_{\mathrm{F}}(t) \geq 0$. The feed suspension contains solids of species 1 to N at the corresponding volume fractions $\phi_1^{\mathrm{F}}(t)$ to $\phi_N^{\mathrm{F}}(t)$. At $x = 0$, the feed flow divides into an upwards- and a downwards-directed bulk flow. We assume that the underflow volume rate $Q_{\mathrm{R}}(t) \geq 0$ is also prescribed, and that $Q_{\mathrm{R}}(t) \leq Q_{\mathrm{F}}(t)$. Consequently, the signed volume rate of the upwards-directed bulk flow is

$$Q_{\mathrm{L}}(t) = Q_{\mathrm{R}}(t) - Q_{\mathrm{F}}(t) \leq 0. \tag{27}$$

An overflow opening is located at depth $x = -1$. Summarizing, we prescribe the volume rates $Q_{\mathrm{F}}(t)$ and $Q_{\mathrm{R}}(t)$ and the feed concentrations $\phi_1^{\mathrm{F}}(t)$ to $\phi_N^{\mathrm{F}}(t)$ as independent control variables. From these we calculate the dependent control variable $Q_{\mathrm{L}}(t)$ by (27).

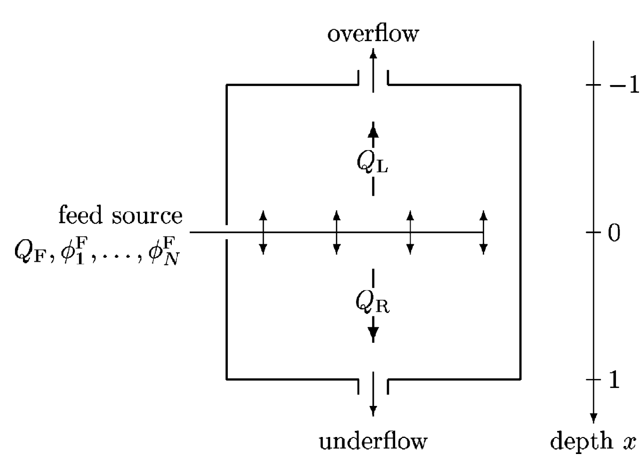

Fig. 7. An idealized, continuously operated clarifier-thickener unit with the flow variables for operation with a polydisperse suspension.

For simplicity, we assume that all control variables are constant with respect to t, and we introduce $q_c := Q_c/S$, $c \in \{\mathrm{F, L, R}\}$. Disregarding for a moment the presence of a solids source but appropriately taking into account these bulk-flow velocities, we can write the flux function for species i as

$$\tilde{g}_i(\Phi, x) = \begin{cases} (q_R - q_F)\phi_i & \text{for } x \le -1, \\ (q_R - q_F)\phi_i + f_i^{\mathrm{M}}(\Phi) & \text{for } -1 < x \le 0, \\ q_R\phi_i + f_i^{\mathrm{M}}(\Phi) & \text{for } 0 < x \le 1, \\ q_R\phi_i & \text{for } x > 1. \end{cases} \tag{28}$$

Including the feed mechanism now leads to the system of conservation laws with source term

$$\frac{\partial \phi_i}{\partial t} + \frac{\partial}{\partial x}\tilde{g}(\Phi, x) = q_F\phi_i^{\mathrm{F}}\delta(x), \quad i = 1, \ldots, K, \tag{29}$$

where $\delta(\cdot)$ denotes the Dirac direct mass. Including the singular source term into the flux function and using the Heaviside function $H(\cdot)$ leads to the equation:

$$\frac{\partial \phi_i}{\partial t} + \frac{\partial}{\partial x}(\tilde{g}_i(\Phi, x) - q_F\phi_i^{\mathrm{F}} H(x)) = 0, \quad i = 1, \ldots, K. \tag{30}$$

Adding the constant $-(q_R - q_F)\phi_i^{\mathrm{F}}$ to the flux term, we can finally state the initial-value problem of interest as

$$\frac{\partial \phi_i}{\partial t} + \frac{\partial}{\partial x}g_i(\Phi, x) = 0, \quad t > 0, \quad -\infty < x < \infty \tag{31}$$

$$\phi_i(x, 0) = \phi_i^0(x), \quad -\infty < x < \infty, \tag{32}$$

$$g(\Phi, x) = \begin{cases} (q_R - q_F)(\phi_i - \phi_i^{\mathrm{F}}) & \text{for } x \le -1, \\ (q_R - q_F)(\phi_i - \phi_i^{\mathrm{F}}) + f_i^{\mathrm{M}}(\Phi) & \text{for } -1 < x \le 0, \\ q_R(\phi_i - \phi_i^{\mathrm{F}}) + f_i^{\mathrm{M}}(\Phi) & \text{for } 0 < x \le 1, \\ q_R(\phi_i - \phi_i^{\mathrm{F}}) & \text{for } x > 1. \end{cases} \tag{33}$$

Note that the flux depends discontinuously on x. The decisive problem is, of course, the appropriate description and discretization of the singular feed source term, and the discontinuous transition between upwards- and downwards-directed flows. Nasr-El-Din et al. [73–75] assume that a feed point source is associated with a "source zone" of finite height within the clarifier-thickener. The obvious purpose of this zone is to act as a "buffer" between the upwards- and downwards-directed bulk flows, so that these flows occur in regions that are spatially separated. In fact, it is assumed in [74] (similar statements occur in [73,75]) that "the solids and the carrier fluid are allowed to exit through the overflow or the underflow boundaries, but they are not allowed to enter the source zone except through the feed stream". However, these assumptions are not put in mathematical terms in [73–75]. Moreover, a model in which the clarification and thickening zones are not connected is clearly unable to explain the really interesting cases, which occur for example if solids accumulate in the thickening zone, form a rising sediment layer, and eventually break through the feed level ($x = 0$). (Papers [73–75] are concerned with polydisperse suspensions, but the shortcomings of the "source zone" concept are independent of the aspect of polydispersivity.)

We present here one numerical example from [72] and consider a bidisperse suspension of polysterene particles ($d_1 = 3.9 \times 10^{-4}$ m, $\rho_1 = 1050\,\mathrm{kg/m^3}$) and glass beads ($d_2 = 1.37 \times 10^{-4}$ m, $\rho_2 = 2850\,\mathrm{kg/m^3}$) suspended in a salt solution ($\rho_\mathrm{f} = 1120\,\mathrm{kg/m^3}$, $\mu_\mathrm{f} = 1.41 \times 10^{-3}$ Pa s). For monodisperse suspensions of each particle species, the hindered settling factor (13) was found to be suitable with the exponents $n = n_1 = 5.705$ and $n = n_2 = 5.826$, respectively. The remaining parameters are $\delta_2 = (d_2/d_1)^2 = 0.1234$, $\rho_1 - \rho_\mathrm{f} = -70\,\mathrm{kg/m^3}$, $\rho_2 - \rho_\mathrm{f} = 1730\,\mathrm{kg/m^3}$ and $\mu = 5.879 \times 10^{-5}\,\mathrm{m^4/(kg\,s)}$. Thus, we are dealing with a heavy-buoyant system. We here use (13) with $\phi_{\max} = 0.7$ and $n = (n_1 + n_2)/2 = 5.765$. The MLB model for this case predicts an appreciable instability (ellipticity) region (see Fig. 8).

The equipment used in [74] is a cylindrical clarifier-thickener of total height 40 cm. The feed source, located in the middle, has a rectangular cross-sectional area $S = 4.24 \times 10^{-4}\,\mathrm{m^2}$. Nasr-El-Din et al. [74] report experiments with many different feed and discharge fluxes. We consider here just the case of $Q_\mathrm{F} = 4.4\,\mathrm{cm^3/s}$, the "split ratio" 75%, i.e., $q_\mathrm{R} = 7.783 \times 10^{-3}$ m/s and $q_\mathrm{L} = -2.594 \times 10^{-3}$ m/s. The feed concentrations are $\phi_1^\mathrm{F} = 0.065$ and $\phi_2^\mathrm{F} = 0.067$.

Fig. 9 shows the numerical simulations of these cases produced by a variant of the Kurganov–Tadmor scheme [53]. We observe that a stationary solution is assumed, and that the heavy species 2 does not enter the clarification zone. No ellipticity region appears in the numerical simulation (Fig. 9) and, for that case, no instabilities were observed experimentally [74].

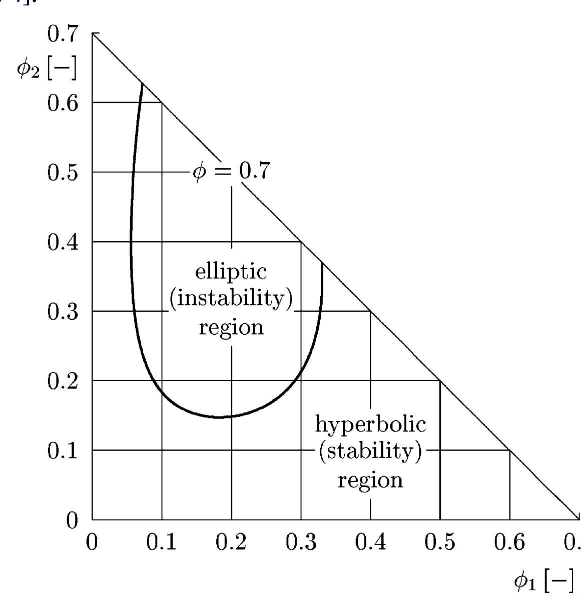

Fig. 8. The instability region for the MLB model and a bidisperse suspension studied by Nasr-El-Din et al. [74].

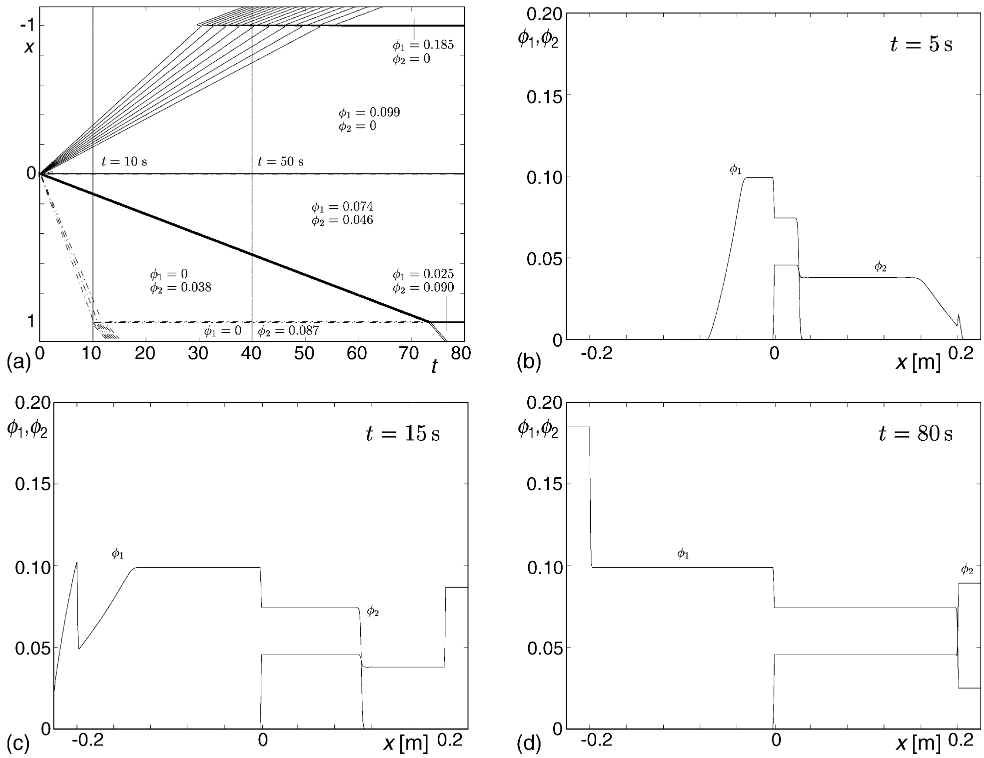

Fig. 9. Simulation of the continuous separation of a bidisperse suspension of buoyant (species 1) and heavy (species 2) particles [72]. Top left: iso-concentration lines and areas of constant composition, top right and bottom: concentration profiles at three selected times.

8. Discussion

We have already noted that Batchelor did not consider hydrodynamic diffusion in his derivation of velocities in polydisperse suspensions. Even if the Batchelor–Wen results were modified to take this into account, there is no justification for extending them to higher concentrations. Batchelor considered only two-particle interactions. This is appropriate for very dilute suspensions, but not for suspensions in which the spheres are close together. For moderately concentrated suspensions, three- and four-particle interactions are important [76,77]. For very concentrated suspensions, lubrication terms must be considered [61]. Thus, any extension of Batchelor's work to higher concentrations is strictly empirical.

It seems to us that models based on slip velocities have an inherent advantage over those based on an extension of Batchelor's equations. At low Reynolds number, all particle–particle interactions occur via the fluid [33]. As indicated by Eq. (7), the gravitational force on a sphere is balanced by the force exerted on it by the fluid. Eq. (4) shows that the upward flow of fluid is substantial when ϕ is large. Thus, it makes sense to use slip velocities to calculate settling velocities. More importantly (as noted in Section 3), the difference between two velocities is objective, while a single velocity is not [38]. The assumptions involved in the derivation of the MLB equation are carefully set out in [33].

A recent review [35] compares results computed from many settling models with data from a paper by Selim et al. [78], which was based, in part, on the work of Smith [79] and Mirza and Richardson [80]. All of these papers predate the advent of shock-capturing methods. Consequently, they use (18) or its generalization to compute ϕ_i. Data from Lockett and Al-Habbooby [81] were not used by Selim et al. They state that "Smith's binary data totalled 85 points and Mirza and Richardson's data consisted of 45 data points, all of which are used here. Lockett and Al-Habbooby's sedimentation data concerned the *initial* sedimentation rates for binary suspensions and could not be used with the present model which uses *average* settling rates" (our emphasis). As noted in Section 5, the propagation of concentration gradients can change the concentration at the top of the region just above the packed bed and subsequently change the concentrations in the upper levels [34]. The reference to average rates suggests that concentration changes were indeed occurring. Certainly, suspensions with voidage values in much of the range shown in Figs. 3–13 of [78] are well known to produce concentration gradients in monodisperse suspensions [48]. Simulations of bidisperse and polydisperse suspensions also produce gradients over a wide range of concentrations. For example, Fig. 10 shows the results of a simulation [82] of the sedimentation of the polydisperse suspension studied by Shannon et al. [4,46] whose experimental values are also indicated. Spheres of 11 species (approximating a normal distribution with 2,048,000 spheres) were randomly distributed over the height of the column and their trajectories were calculated by the method of Bargieł et al. [34] (which is summarized in Section 5). Note

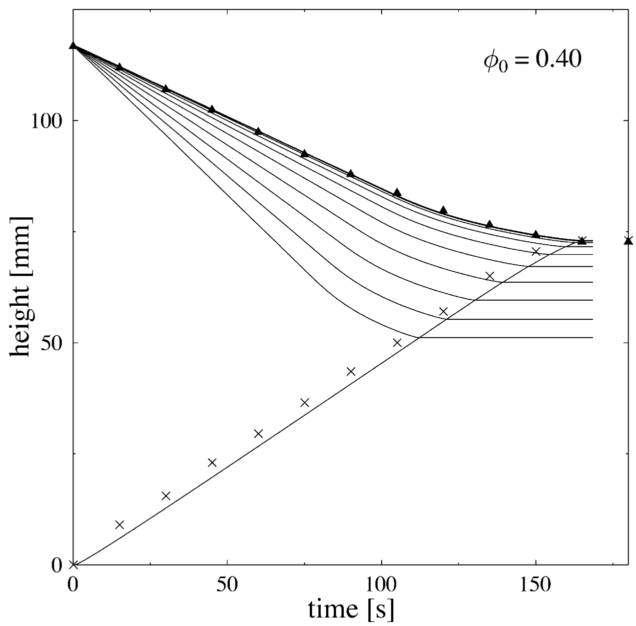

Fig. 10. Simulation of the sedimentation of a polydisperse suspension. Each upper line represents the path of the top sphere of a species. The "Smith effect" and the very small volume of the two smallest species cause the uppermost lines to be very close together. The line from the origin is the position of the top of the packed bed.

that these paths, which are initially straight, become strongly curved as concentration gradients are propagated upwards from the bottom. Thus, it is possible that the voidage values shown in the figures in [78] are purely nominal and not those that actually determine the settling velocities.

This emphasizes the importance of shock-capturing [53] and simulation [34] methods that avoid these difficulties.

Concerning the numerical results shown in Section 7, it should be pointed out that the use of the Kurganov–Tadmor scheme (or of any other scheme) for a *system* of conservation laws is not supported by a rigorous convergence theory. In particular, the question of a meaningful solution concept for hyperbolic-elliptic systems, such as those appearing in Sections 7.2 and 7.3, is still open. The use of these schemes as simulation tools is essentially based on experience.

Acknowledgement

We acknowledge support by the Collaborative Research Center (Sonderforschungsbereich) 404 at the University of Stuttgart. RB acknowledges support by Fondecyt project 1050728 and fondap in Applied Mathematics.

References

[1] E.M. Tory, D.K. Pickard, A three-parameter Markov model for sedimentation, Can. J. Chem. Eng. 55 (1977) 655–665.

[2] M.A. Al-Naafa, M.S. Selim, Sedimentation of monodisperse and bidisperse hard-sphere colloidal suspensions, AIChE J. 38 (1992) 1618–1630.

[3] E.M. Tory, M.T. Kamel, Mean velocities in polydisperse suspensions, Powder Technol. 93 (1997) 199–207.

[4] P.T. Shannon, E. Stroupe, E.M. Tory, Batch and continuous thickening. Basic theory. Solids flux for rigid spheres, Ind. Eng. Chem. Fund. 2 (1963) 203–211;
P.T. Shannon, E. Stroupe, E.M. Tory, Correction, Ind. Eng. Chem. Fund. 3 (1964) 184.

[5] R.H. Davis, M.A. Hassen, Spreading of the interface at the top of a slightly polydisperse sedimenting suspension, J. Fluid Mech. 196 (1988) 107–134.

[6] R.H. Davis, K.H. Birdsell, Hindered settling of semidilute monodisperse and polydisperse suspensions, AIChE J. 34 (1988) 123–129.

[7] J. Happel, H. Brenner, Low Reynolds Number Hydrodynamics, Nijhoff, Dordrecht, The Netherlands, 1983.

[8] C.S. Robinson, Some factors influencing sedimentation, Ind. Eng. Chem. 18 (1926) 869–871.

[9] W.O. Kermack, A.G. M'Kendrick, E. Ponder, The stability of suspensions. III. The velocities of sedimentation and of cataphoresis of suspensions in a viscous fluid, Proc. Roy. Soc. Edinburgh 49 (1929) 170–197.

[10] G.K. Batchelor, Sedimentation in a dilute dispersion of spheres, J. Fluid Mech. 52 (1972) 245–268.

[11] H.H. Steinour, Rate of sedimentation. Non-flocculated suspensions of uniform spheres, Ind. Eng. Chem. 36 (1944) 618–624.

[12] J.F. Richardson, W.N. Zaki, Sedimentation and fluidization I, Trans. Inst. Chem. Eng. (London) 32 (1954) 35–53.

[13] E. Barnea, J. Mizrahi, A generalized approach to the fluid dynamics of particulate systems. Part 1. General correlation for fluidization and sedimentation in solid multiparticle systems, Chem. Eng. J. 5 (1973) 171–189.

[14] K.J. Scott, W.G.B. Mandersloot, The mean particle size in hindered settling of multisized particles, Powder Technol. 24 (1979) 99–101.

[15] K.J. Scott, Hindered settling of a suspension of spheres. Critical evaluation of equations relating settling rate to mean particle diameter and suspension concentration, CSIR Report CENG 497, Chemical Engineering Research Group, Council for Scientific and Industrial Research, Pretoria, South Africa, 1984.

[16] D.R. Oliver, The sedimentation of suspensions of closely sized spherical particles, Chem. Eng. Sci. 15 (1961) 230–242.

[17] D.K. Pickard, E.M. Tory, A Markov model for sedimentation, J. Math. Anal. Appl. 60 (1977) 349–369.

[18] J.M. Ham, G.M. Homsy, Hindered settling and hydrodynamic dispersion in quiescent sedimenting suspensions, Int. J. Multiphase Flow 14 (1988) 533–546.

[19] G.K. Batchelor, Sedimentation in a dilute polydisperse system of interacting spheres. Part 1. General theory, J. Fluid Mech. 119 (1982) 379–408.

[20] G.K. Batchelor, C.S. Wen, Sedimentation in a dilute polydisperse system of interacting spheres. Part 2. Numerical results, J. Fluid Mech. 124 (1982) 495–528.

[21] E.J. Hinch, Sedimentation of small particles, in: E. Guyon, J.P. Nadal, Y. Pomeau (Eds.), Disorder and Mixing, Kluwer Academic Publishers, Dordrecht, 1988, p. 153.

[22] B.H. Kaye, R.P. Boardman, Cluster formation in dilute suspensions, in: Proceedings of the Symposium on Interactions between Fluids and Particles,, Instn. Chem. Eng., London, June 20–22, 1962, pp. 17–21.

[23] B. Koglin, Experimentelle Untersuchungen zur Sedimentation von Teilchenkomplexen in Suspensionen, Chem. Eng. Technol. 44 (1972) 515–521.

[24] G. Bickert, W. Stahl, Sedimentation behaviour of mono- and polydisperse submicron particles in dilute and in concentrated suspensions, in: Proceedings of the Seventh World Filtration Congress, vol. I, Budapest, Hungary, May 20–23, 1996, pp. 141–145.

[25] E.M. Tory, M.T. Kamel, C.F. Chan Man Fong, Sedimentation is container-size dependent, Powder Technol. 73 (1992) 219–238.

[26] B. Koglin, Zum Mechanismus der Sinkgeschwindigkeitserhöhung in niedrig konzentrierten Suspensionen, in: Proceedings of the First European Symposium on Particle Size Measurement, Nuremberg, 1975. Dechema Monographs, nos. 1589–1615, vol. 79, part B, Verlag Chemie GmbH, Weinheim, Bergstraße,, 1976, pp. 235–250.
[27] U. Geigenmüller, P. Mazur, Sedimentation of homogeneous suspensions in finite vessels, J. Stat. Phys. 53 (1988) 137–173.
[28] R.-H. Jean, L.-S. Fan, On the model equations of Gibilaro and Foscolo with corrected buoyancy force, Powder Technol. 72 (1982) 201–205.
[29] R.H. Davis, H. Gecol, Hindered settling function with no empirical parameters for polydisperse suspensions, AIChE J. 40 (1994) 570–575.
[30] J.F. Richardson, F.A. Shabi, The determination of concentration distribution in a sedimenting suspension using radioactive solids, Trans. Inst Chem. Eng. 38 (1960) 33–42.
[31] J.H. Masliyah, Hindered settling in a multi-species particle system, Chem. Eng. Sci. 34 (1979) 1166–1168.
[32] M.J. Lockett, K.S. Bassoon, Sedimentation of binary particle mixtures, Powder Technol. 24 (1979) 1–7.
[33] R. Bürger, K.H. Karlsen, E.M. Tory, W.L. Wendland, Model equations and instability regions for the sedimentation of polydisperse suspensions of spheres, Z. Angew. Math. Mech. 82 (2002) 699–722.
[34] M. Bargieł, R.A. Ford, E.M. Tory, Simulation of sedimentation of polydisperse suspensions. A particle-based approach, AIChE J., in press.
[35] A. Zeidan, S. Rohani, A. Bassi, P. Whiting, Review and comparison of solids settling velocity models, Rev. Chem. Eng. 19 (2003) 473–530.
[36] S. Berres, R. Bürger, K.H. Karlsen, E.M. Tory, Strongly degenerate parabolic–hyperbolic systems modeling polydisperse sedimentation with compression, SIAM J. Appl. Math. 64 (2003) 41–80.
[37] V.S. Patwardhan, C. Tien, Sedimentation and liquid fluidization of solid particles of different sizes and densities, Chem. Eng. Sci. 40 (1985) 1051–1060.
[38] D.A. Drew, S. Passman, Theory of Multicomponent Fluids, Springer-Verlag, New York, 1999.
[39] Z. Ha, S. Liu, Settling velocities of polydisperse concentrated suspensions, Can. J. Chem. Eng. 80 (2002) 783–790.
[40] E.M. Tory, R.A. Ford, Simulation of sedimentation of bidisperse suspensions, Int. J. Miner. Process. 73 (2004) 119–130.
[41] Y.P. Fessas, R.H. Weiland, Convective solids settling induced by a buoyant phase, AIChE J. 27 (1981) 588–592.
[42] Y.P. Fessas, R.H. Weiland, The settling of suspensions promoted by rigid buoyant particles, Int. J. Multiphase Flow 10 (1985) 485–507.
[43] R.H. Weiland, Y.P. Fessas, B.V. Ramarao, On instabilities arising during sedimentation of two-component mixture of solids, J. Fluid Mech. 142 (1984) 383–389.
[44] G.K. Batchelor, R.W. Janse van Rensburg, Structure formation in bidisperse sedimentation, J. Fluid Mech. 119 (1986) 379–407.
[45] P.M. Biesheuvel, H. Verweij, V. Breedveld, Evaluation of instability criterion for bidisperse sedimentation, AIChE J. 47 (2001) 45–52.
[46] P.T. Shannon, R.D. DeHaas, E.P. Stroupe, E.M. Tory, Batch and continuous thickening. Prediction of batch settling behavior with results for rigid spheres, Ind. Eng. Chem. Fund. 3 (1964) 250–260.
[47] G.J. Kynch, A theory of sedimentation, Trans. Faraday. Soc. 48 (1952) 166–176.
[48] M.C. Bustos, F. Concha, R. Bürger, E.M. Tory, Sedimentation and Thickening, Kluwer Academic Publishers, Dordrecht, 1999.
[49] R. Bürger, E.M. Tory, On upper rarefaction waves in batch settling, Powder Technol. 108 (2000) 74–87.
[50] T.N. Smith, The sedimentation of particles having a dispersion of sizes, Trans. Inst. Chem. Eng. 44 (1966) T153–T157.
[51] E.M. Tory, R.A. Ford, M. Bargieł, Simulation of sedimentation of monodisperse and polydisperse suspensions, in: M.A Efendiev, W.L. Wendland (Eds.), Analysis and Simulation of Multifield Problems, Lecture Notes in Applied and Computational Mechanics, vol.12, Springer-Verlag, Berlin, 2003, pp. 343–348.
[52] R. Bürger, K.-K. Fjelde, K. Höfler, K.H. Karlsen, Central difference solutions of the kinematic model of settling of polydisperse suspensions and three-dimensional particle-scale simulations, J. Eng. Math. 41 (2001) 167–187.
[53] A. Kurganov, E. Tadmor, New high resolution central schemes for nonlinear conservation laws and convection–diffusion equations, J. Comp. Phys. 160 (2000) 241–282.
[54] H. Nessyahu, E. Tadmor, Non-oscillatory central differencing for hyperbolic conservation laws, J. Comp. Phys. 87 (1990) 408–463.
[55] B. Xue, Y. Sun, Modeling of sedimentation of polydisperse spherical beads with a broad size distribution, Chem. Eng. Sci. 58 (2003) 1531–1543.
[56] E. Tadmor, Approximate solutions of nonlinear conservation laws, in: B. Cockburn, C. Johnson, C.-W. Shu, E. Tadmor (Eds.), Advanced Numerical Approximation of Nonlinear Hyperbolic Equations (Cetraro, Italy, 1997), Lecture Notes in Mathematics, vol. 1697, Springer-Verlag, Berlin, 1998, pp. 1–149.
[57] R.J. Le Veque, Finite Volume Methods for Hyperbolic Problems, Cambridge University Press, Cambridge, UK, 2002.
[58] G.D.M. MacKay, S.G. Mason, Approach of a solid sphere to a rigid plane interface, J. Colloid Sci. 16 (1961) 632–635.
[59] G.D.M. MacKay, M. Suzuki, S.G. Mason, Approach of a solid sphere to a rigid plane interface. Part 2, J. Colloid Sci. 18 (1963) 103–104.
[60] H. Brenner, The slow motion of a sphere through a viscous fluid towards a plane surface, Chem. Eng. Sci. 16 (1961) 242–251.
[61] S. Kim, S.J. Karrila, Microhydrodynamics: Principles and Selected Applications, Butterworth-Heinemann, Boston, 1991.
[62] S. Berres, R. Bürger, E.M. Tory, Mathematical model and numerical simulation of the liquid fluidization of polydisperse solid particle mixtures, Comput. Visual. Sci. 6 (2004) 67–74.
[63] S. Berres, R. Bürger, E.M. Tory, On mathematical models and numerical simulation of the fluidization of polydisperse suspensions, Appl. Math. Model. 29 (2005) 159–193.
[64] N. Epstein, B.P. Leclair, B.B. Pruden, Liquid fluidization of binary particle mixtures. II. Bed inversion, Chem. Eng. Sci. 40 (1985) 1517–1526.
[65] L.G. Gibilaro, R. Di Felice, S.P. Waldram, P.U. Foscolo, A predictive model for the equilibrium composition and inversion of binary-solid liquid fluidized beds, Chem. Eng. Sci. 41 (1986) 379–387.
[66] H. Moritomi, T. Iwase, T. Chiba, A comprehensive interpretation of solid layer inversion in liquid fluidized beds, Chem. Eng. Sci. 37 (1982) 1751–1757.
[67] H. Moritomi, T. Yamagishi, T. Chiba, Prediction of complete mixing of liquid–fluidized binary solid particles, Chem. Eng. Sci. 41 (1986) 297–305.
[68] R. Bürger, F. Concha, K.-K. Fjelde, K.H. Karlsen, Numerical simulation of the settling of polydisperse suspensions of spheres, Powder Technol. 113 (2000) 30–54.
[69] S. Berres, R. Bürger, On gravity and centrifugal settling of polydisperse suspensions forming compressible sediments, Int. J. Solids Struct. 40 (2003) 4965–4987.
[70] G. Anestis, Eine eindimensionale Theorie der Sedimentation in Absetzbehältern veränderlichen Querschnitts und in Zentrifugen, Doctoral Thesis, Technical University of Vienna, Austria, 1981.
[71] G. Anestis, W. Schneider, Application of the theory of kinematic waves to the centrifugation of suspensions, Ing. Arch. 53 (1983) 399–407.
[72] S. Berres, R. Bürger, K.H. Karlsen, Central schemes and systems of conservation laws with discontinuous coefficients modeling gravity separation of polydisperse suspensions, J. Comp. Appl. Math. 164–165 (2004) 53–80.
[73] H. Nasr-El-Din, J.H. Masliyah, K. Nandakumar, Continuous gravity separation of concentrated bidisperse suspensions in a vertical column, Chem. Eng. Sci. 45 (1990) 849–857.

[74] H. Nasr-El-Din, J.H. Masliyah, K. Nandakumar, Continuous separation of suspensions containing light and heavy particle species, Can. J. Chem. Eng. 77 (1999) 1003–1012.
[75] H. Nasr-El-Din, J.H. Masliyah, K. Nandakumar, D.H.-S. Law, Continuous gravity separation of a bidisperse suspension in a vertical column, Chem. Eng. Sci. 43 (1988) 3225–3234.
[76] P. Mazur, W. van Saarloos, Many-sphere hydrodynamic interactions and mobilities in a suspension, Physica A 115 (1982) 21–57.
[77] M.T. Kamel, E.M. Tory, Sedimentation of clusters of identical spheres. I. Comparison of methods for computing velocities, Powder Technol. 59 (1989) 227–248;
M.T. Kamel, E.M. Tory, Erratum, Powder Technol. 94 (1997) 266.
[78] M.S. Selim, A.C. Kothari, R.M. Turian, Sedimentation of multi-sized particles in concentrated suspensions, AIChE J. 29 (1983) 1029–1038.
[79] T.N. Smith, The differential sedimentation of particles of two different species, Trans. Inst. Chem. Eng. 43 (1965) T69–T73.
[80] S. Mirza, J.F. Richardson, Sedimentation of suspensions of particles of two or more sizes, Chem. Eng. Sci. 34 (1979) 447–454.
[81] M.J. Lockett, H.M. Al-Habbooby, Differential settling by size of two particle species in a liquid, Trans. Inst. Chem. Eng. 51 (1973) 281–292.
[82] M. Bargieł, private communication, March 13, 2003.